RvD1binding with FPR2 attenuates inflammation via Rac1/NOX2 pathway after neonatal hypoxic-ischemic injury in rats

Wei Liu[a,b], **Juan Huang**[b,c], **Desislava Doycheva**[b], **Marcin Gamdzyk**[b], **Jiping Tang**[b], **John H. Zhang**[b,*]

[a]Department of Physiology, School of Basic Medical Science, Guangzhou University of Chinese Medicine, Guangzhou 510006, China

[b]Department of Physiology and Pharmacology, Basic Sciences, School of Medicine, Loma Linda, CA, 92354, USA

[c]Institute of Neuroscience, Chongqing Medical University, Chongqing, 40016, China

Abstract

Neuroinflammation plays a crucial role in the pathological development after neonatal hypoxia-ischemia (HI). Resolvin D1 (RvD1), an agonist of formyl peptide receptor 2 (FPR2), has been shown to exert anti-inflammatory effects in many diseases. The objective of this study was to explore the protective role of RvD1 through reducing inflammation after HI and to study the contribution of Ras-related C3 botulinum toxin substrate 1 (Rac1)/nicotinamide adenine dinucleotide phosphate (NADPH) oxidase 2 (NOX2) pathways in RvD1-mediated protection. Rat pups (10-day old) were subjected to HI or sham surgery. RvD1 was administrated by intraperitoneal injection 1 h after HI. FPR2 small interfering ribonucleic acid (siRNA) and Rac1 activation CRISPR were administered prior to RvD1 treatment to elucidate the possible mechanisms. Time course expression of FPR2 by Western blot and RvD1 by ELISA were conducted at 6 h, 12 h, 24 h, 48 h and 72 h post HI. Infarction area, short-term neurological deficits, immunofluorescent staining and Western blot were conducted at 24 h post HI. Long-term neurological behaviors were evaluated at 4 weeks post HI. Endogenous expression levels of RvD1 decreased in time dependent manner while the expression of FPR2 increased after HI, peaking at 24 h post HI. Activation of FPR2, with RvD1, reduced percent infarction area, and alleviated short- and long-term neurological deficits. Administration of RvD1 attenuated inflammation after HI, while, either inhibition of FPR2 with siRNA or activation of Rac1 with CRISPR reversed those effects. Our results showed that RvD1 attenuated neuroinflammation through FPR2, which then interacted with Rac1/NOX2 signaling pathway, thereby reducing infarction area and

[*]Corresponding author at: Department Anesthesiology and Basic Sciences, Loma Linda University, School of Medicine, 11041 Campus Street, Risley Hall, Loma Linda, CA, 92354, USA. jhzhang@llu.edu.

alleviating neurological deficits after HI in neonatal rat pups. RvD1 may be a potential therapeutic approach to reduce inflammation after HI.

1. Introduction

Neonatal hypoxic-ischemic (HI) encephalopathy (HIE), with the occurrence of 1.5-2‰ in developed countries and 26‰ in undeveloped areas, is a worldwide leading cause for neonatal morbidity and mortality (Kurinczuk et al., 2010; Parikh and Juul, 2018). As a result of a reduction in oxygen and glucose to the brain, some infants suffer from severe neurological disorders, such as cerebral palsy, cognitive and intellectual deficits, and behavioral problems (Lapchak and Zhang, 2017). To date, hypothermia is the most effective intervention for HIE (Dixon et al., 2015). However, it has some adverse effects, such as sinus bradycardia and thrombocytopenia. Despite its effectiveness, some newborns that seem to adequately recover have shown seizure activity later in life (McAdams and Juul, 2016). Therefore, there is a great need to investigate novel strategies to protect the neonatal brain after HIE.

Inflammation is increasingly recognized as a critical pathogenic factor of neonatal brain damage (Ziemka-Nalecz et al., 2017). It has been shown that after HI, microglia and astrocytes are activated within minutes resulting in the large release of pro-inflammatory cytokines, such as TNF-α and IL-1β (Tuttolomondo et al., 2008). These pro-inflammatory cytokines promote both apoptosis and necrosis of neurons, impair neurological functions, and inhibit neurogenesis (Ziemka-Nalecz et al., 2017). If acute inflammation is not resolved properly, it will hinder the proper development of the brain, leading to various dysfunctions.

Formyl peptide receptor 2 (FPR2), also termed as formyl peptide receptor like 1 (FPRL1) or lipoxin A4 (LXA4) receptor, is a G protein-coupled chemoattractant receptor that plays an important roles in resolving inflammation (He and Ye, 2017). Among formyl peptide receptors, FPR2 is widely distributed in the brain and especially functionally expressed in microglia and astrocytes (Gavins, 2010). The binding of FPR2 to its endogenous ligand, resolvin D1 (RvD1), has been shown to have anti-inflammatory mechanisms (Serhan and Chiang, 2008). Moreover, administration of RvD1 exerted anti-inflammatory effects in hemicerebellectomy (HCb)-lesioned rats (Bisicchia et al., 2018). However, the potential role of FPR2 activation against neuroinflammation after neonatal HI has yet to be determined.

NOX2 has been widely recognized for production of reactive oxygen species (ROS). However, in recent years, mounting evidence has demonstrated that NOX2 is involved in inflammation (Pang et al., 2018). Arecent study demonstrated thatNOX2 inhibition showed to be neuroprotective against inflammatory cytokine-mediated brain damage (Chen et al., 2011). A previous study indicated that RvD1 inactivated NOX2 in macrophages (Lee and Surh, 2013). Ras-related C3 botulinum toxin substrate 1 (Rac1) has been emerging as a new pharmacological target of cerebrovascular diseases and plays critical role in cerebral

ischemia in rats (Carrizzo et al., 2014; Raz et al., 2010). In addition, FPR2 activation was able to suppress TNF-α induced inflammatory response via inhibition of Rac1 (Peshavariya et al., 2013). Numerous studies reported that NOX activation needed active Rac1, and NOX2 was decreased when Rac1 was knocked down (Acevedo and González-Billault, 2018; Akbar et al., 2018).

Based on the above evidence, we hypothesized that FPR2 agonist, RvD1, attenuated inflammation via inhibition of Rac1/NOX2, leading to attenuation of inflammation and improvement of neurological function in a rat model of neonatal HI.

2. Methods and materials

2.1. Animals

All experiments were approved by the Institutional Animal Care and Use Committee of Loma Linda University. All studies were conducted in accordance with the United States Public Health Service's Policy on Humane Care and Use of Laboratory Animals. Sprague Dawley rat mothers with litters of 10-12 pups were purchased from Envigo (Livermore, CA). Ten-day old rat pups were used for this study. All animal tests were conducted blindly. All animal experiments comply with animal research: reporting in vivo experiments (ARRIVE) guidelines.

2.2. Experimental Design

2.2.1.   Experiment 1—To determine the time course of FPR2 expression and endogenous RvD1 concentration after HI, 36 rat pups were randomly divided into six groups: sham, 6 h after HI, 12 h after HI, 24 h after HI, 48 h after HI, and 72 h after HI (n=6 per group). Western blot analysis was used to detect FPR2 expression and ELISA was used for RvD1 concentration.

2.2.2.   Experiment 2—To evaluate the effects of RvD1 on percent infarction area, short-term neurological behavior and to determine the best dose of RvD1, 30 rat pups were randomly divided into five groups (n=6 per group): sham, HI+vehicle, HI+RvD1 (1 μg/kg), HI+RvD1 (5 μg/kg), HI+RvD1 (15 μg/kg). Geotaxis reflex was performed to detect short-term neurological functions, and weight changes were also observed. TTC staining was conducted to detect the infarction area.

To assess the function of RvD1 on long-term neurological behavior after HI, 36 rat pups were randomly separated into three groups: sham, HI+vehicle, and HI+RvD1 (best dose) (n=12 per group). Foot fault test, rotarod test and morris water maze test were conducted at 4 weeks after HI.

2.2.3.   Experiment 3—Double immunofluorescent staining was conducted for localization of FPR2 with Iba1 (microglial marker) and GFAP (astrocytic marker). Moreover, to explore the effect of RvD1 on inflammation, cell morphology of glial cells were observed, and immunofluorescent density of Iba1, GFAP, MPO (indicator of inflammation) (Fathali et al., 2013) and IL-1β (representative inflammatory cytokines) were quantified (n=3 for each group).

2.2.4.   Experiment 4—To investigate the underlying mechanism of RvD1 mediated anti-inflammatory effects after HI, FPR2 siRNA and Rac1 activation CRISPR were administered by intracerebroventricular (i.c.v.) injection at 48 h before HI surgery separately, then followed by RvD1 treatment 1 h after HI. The following groups were included (n=6 for each group): sham, HI+vehicle, HI+RvD1, HI+RvD1+FPR2 siRNA, HI+RvD1+control siRNA, HI+RvD1+Rac1 CRISPR, HI+RvD1+control CRISPR.

2.3. HI surgery

Rice-Vannucci neonatal HI model was induced as previously described (Ye et al., 2018). After the pups were anesthetized with 3% isoflurane, the right common carotid artery (CCA) was gently isolated, double ligated and cut between the two ligation sites. Rats were allowed to recover 1 h on a heated blanket after which they were exposed to hypoxia (8% oxygen and 92% nitrogen) for 2 h and 30 min at 37 °C. After that rat pups were returned to their mothers. For the sham operated animals, CCA was isolated and exposed but without ligation and hypoxia.

2.4. Drug administration

RvD1 (Caymen, USA) as a selective agonist of FPR2, was dissolved in saline and tested with three different doses (1 μg/kg 5 μg/kg, 15 μg/kg), which were given intraperitoneally (i.p.) 1 h after HI. Saline was used as vehicle for RvD1.

2.5. Intracerebroventricular injection

FPR2 siRNA and scramble siRNA (Dharmacon, USA; 2 μl, 300pmol/μl) were administered (i.c.v.) to the ipsilateral hemisphere 48 h before HI. Briefly, The ICV injections were performed at 1.5mm posterior, 1.5mm lateral to the bregma and 2.5mm deep from the surface at a rate of 0.5 μl/min. After waiting for 5 min, the needle was removed over 5 min. The burr hole was then sealed with bone wax. 1 μg of Rac1 CRISPR activation plasmid (Santa Cruz, USA) or control CRISPR Activation Plasmid (Santa Cruz, USA) were given via ICV injection as described above at 48 h before HI.

2.6. Infarct area measurements

Rats were deeply anesthetized and perfused transcardially with PBS at 72 h post HI. Brain samples were quickly removed, sectioned into 2 mm slices and immersed into 2% solution of 2,3,5 triphenyltetrazolium chloride (TTC) (Sigma Aldrich, USA). Percent infarct area was measured by Image J software (NIH) and calculated as following: [(total area of contralateral hemisphere)-(un-infarcted area of ipsilateral hemisphere)] / (total area of contralateral hemisphere*2) (Chen et al., 2018, Fan et al., 2017).

2.7. Short-term neurological test

To evaluate short-term neurological function, negative geotaxis test was performed blindly at 24 h post HI. Pups were placed on an inclined board (45°) with the rat pups facing downward. The time needed for the pups to adjust their bodies until head facing the upper of the board was recorded. The maximum time was 60 s.

2.8. Long-term neurological tests

Long-term neurological tests were conducted using foot-fault test, rotarod test and water maze test at 4 weeks post HI. Foot-fault test was used to evaluate motor abilities. Rats were placed on a horizontal grid floor for 1 min, which is 28×3 cm with a mesh size of 4 cm^2. Foot-fault was defined when one of rats' limbs could not be accurately put and fell through the openings in the grid. The whole process for each rat was recorded using a video device, and the number of foot-faults was counted respectively. Special motor impairment was assessed by rotarod test using an accelerating rotating (Columbus Instruments Rotamex, USA). The duration for a rat remaining on the rotarod treadmill was recorded and analyzed. Two rotarod trials accelerating from 5 or 10 rpm were performed separately. Morris water maze test was used to assess memory and learning (Jiang et al., 2017). Cued tests were performed for five consecutive days. On the first day, rats were allowed to swim for maximum of 60s and if they could not discover the hidden platform within the 60s time period, they were manually guided to the platform. Days 2-5 tested the learning and memory abilities of the rats with a submerged platform. On the 6th day, hidden tests were conducted within 60s for each to compare the time spent in the target quadrant. During all experiments rats were tracked with Video Tracking SystemSMART-2000 (San Diego Instruments Inc., CA).

2.9. Brain tissue loss evaluation (nissl staining) and Immunofluorescent staining

Rats were anesthetized and perfused with cold PBS followed by 4% formalin at 24 h post HI. The brains were taken out and post-fixed overnight, then immersed in 30% sucrose until dehydrated and frozen in OCT. Coronal sections were cut at 10 μm thickness using a cryostat (Leica LM3050S). For nissl staining the slides were dehydrated in 95% and 70% ethanol for 1 min respectively, stained with 0.5% cresyl violet (Sigma-Aldrich, USA) for 2 min, and then dehydrated in 100% ethanol and xylene for 1.5 min consecutively. The percentage of brain tissue loss was calculated with the same equation for infarct area.

Immunofluorescent staining was performed as described previously (Ye et al., 2018). Briefly, after being permeabilized with 0.3% Triton X-100 and blocked by 5% donkey serum, sections were incubated with primary antibodies (FPR2, 1:100, Abcam, USA; Iba1, 1:100, Abcam, USA; GFAP, 1:100, Abcam, USA; IL-1β, 1:200, Abcam, USA; MPO, 1:200, Abcam, USA) at 4°C overnight. The next day sections were incubated with appropriate fluorescent dye-conjugated secondary antibodies (1:200) for 2 h at room temperature and mounted using Vectashield Antifade with DAPI (Vector Laboratories Inc., USA). The stained sections were captured under a fluorescence microscope Leica DMi8 (Leica Microsystems, Germany) and analyzed with Image Pro Plus software (Olympus, Melville, NY).

2.10. Tissue collection for ELISA and Western blotting

After HI rats were euthanized deeply with isoflurane and transcardially perfused with cold PBS, brains were quickly removed, and then contralateral and ipsilateral cerebrums were frozen separately in liquid nitrogen. Samples were homogenized with lysis buffer (Santa Cruz Biotechnology, USA) and standing on ice for half an hour. The supernatant were collected after centrifugation and quantified with DC™ Protein Assay (Bio-Rad, USA).

2.11. ELISA for RvD1

RvD1 ELISA kit was purchased from Cayman Chemicals (USA). Operations were conducted according to instructions, briefly incubated overnight at 4°C and developed by Ellman's reagent. The optical densities were measured with a plate reader (Bio-Rad) and concentrations of samples were calculated on the basis of standard curve.

2.12. Western blotting

Western blotting was performed as previously described (Gamdzyk et al., 2018). A total of 30 μg protein, from ipsilateral hemisphere, was loaded and separated by 8%-12% SDS-PAGE gel and then transferred onto nitrocellulose membranes (0.45 μm). The membranes were blocked with 5% non-fat blocking grade milk (Bio-Rad, USA), and incubated overnight at 4°C with primary antibodies (anti-FPR2, 1:500, Abcam, USA; anti-NOX2, 1:500, Abcam, USA; anti-Rac1, 1:2000, Abcam, USA; IL-1β, 1:1000, Abcam, USA; TNF-α, 1:500, Abcam, USA; β-actin, 1:2000, Santa Cruz Biotechnology, USA). The next day, membranes were probed with anti-rabbit (or anti-mouse) secondary antibodies (1:3000 Santa Cruz Biotechnology, USA) for 2 h at room temperature. Finally, the bands were developed with ECL Plus kit (Amersham Bioscience, Arlington Heights, IL, USA) and exposed onto an X-ray film. For quantification, gray values were measured and normalized with the control band by Image J software (National Institutes of Health, USA).

2.13. Rac1 activity assay

The activation form of Rac1 (GTP-Rac1) was obtained by a pull-down assay using Rac1 activation Assay kit (Abcam, USA). According to the instructions, brain lysates were incubated with PAK1 PBD bead at 4°C for 1 h. The eluted proteins were then detected by performing Western blotting with anti-Rac1 antibody (Abcam, USA) as described above.

2.14. Statistics

All animals were randomly assigned to different groups. All Data are expressed as the mean and standard deviation (mean ± SD). Statistical analysis was performed with the software of Graph Pad Prism 7. One-way analysis of variance (ANOVA) followed by multiple comparisons between groups using Tukey's post hoc test was used. $P < 0.05$ was considered to indicate a statistically significant difference.

3. Results

3.1. Time course expression of FPR2 and RvD1

As shown in Fig. 1A, the expression of FPR2 was up-regulated after HI and peaked at 24 h compared with sham group ($P < 0.05$). The levels of endogenous RvD1 were evaluated by ELISA. The data showed that RvD1 was decreased after HI, reaching significance at 24 h post HI ($P < 0.05$, Fig. 1B).

3.2. RvD1 reduced infarct area and improved short-term neurological behavior at 24 h post HI

To determine the best dose of exogenous RvD1 supplement, three doses of RvD1 were used. Infarct area and geotaxis test were conducted at 24 h after HI, since FPR2 was significantly increased at this time point. The data showed that both 5 μg/kg (medium dose) and 15 μg/kg (high dose) of RvD1 significantly reduced percent infarct area, as indicated by TTC staining and improved neurological function as demonstrated by geotaxis reflex when compared with vehicle group (P < 0.05, Fig. 2A–C). In addition, administration of RvD1 at both medium and high doses significantly reduced the weight loss at 24 h after HI (P < 0.05, Fig. 2D). Thus, 5 ug/kg of RvD1 was selected as the optional dose for the long-term effects and mechanism study.

3.3. RvD1 improved long-term neurological function and reduced brain tissue loss at 4 weeks after HI

In the foot fault test, rats in vehicle displayed significantly more foot faults in contralateral limbs compared to the sham group at 4 weeks after HI, while RvD1 markedly improved the performance (P < 0.05, Fig. 3A). As to the rotarod test, rats in vehicle group showed less latency at the speed of 5 PRM and 10 PRM although no difference at constant speed compared to sham group at 4 weeks after HI. Administration with RvD1 significantly prolonged latency at the speed of 5 RPM but no significant difference at 10 RPM when compared with vehicle group (Fig. 3B). For the water maze test conducted from 4 weeks after HI and lasted for 6 consecutive days, rats in vehicle group traveled significantly longer distance and more took longer time to find the platform when compared to sham group. However, RvD1 shortened the distance and escape latency from block 3 and block 4 respectively, indicating that their learning abilities were enhanced (P < 0.05, Fig. 3C, D). In the probe quadrant trial, rats in vehicle group spent less time in probe quadrant when compared to sham group and RvD1 increased the time duration in probe quadrants on the 6th day (P < 0.05, Fig. 3E, F). There was no significant gender difference in response to the treatment, so we merged male and female for analysis. Consistently, HI caused severe brain injury as demonstrated by large portion of brain tissue loss of the ipsilateral hemisphere, while treatment with RvD1 significantly attenuated brain tissue loss (P < 0.05, Fig. 3G, H).

3.4. Localization of FPR2 with microglia and astrocytes and effects of RvD1 on inflammation at 24 h post HI

Double immunofluorescent staining was conducted to localize FPR2 with microglia and astrocytes. As shown in Fig. 4, FPR2 showed to be localized with Iba1 (microglial marker) and GFAP (astrocytic marker) (Fig. 4 A, B). Enhanced activation of microglia and astrocytes was observed (Activated microglia and astrocytes have enlarged cell body and thick branches) and an upregulated expression of Iba1 and GFAP were shown in vehicle group. However, RvD1 attenuated glial activation induced by HI along with decreased Iba1 and GFAP intensity compared with vehicle group (P < 0.05, Fig. 4 C, D)

Since both activated microglia and astrocytes contribute to inflammation, which plays an important role in the pathological development after HI, MPO and IL-1β staining was performed to evaluate the extent of inflammation. As shown in Fig. 4, the level of intensity

of MPO and IL-1β in vehicle group was much higher compared to sham group at 24 h after HI, while administration with RvD1 reversed that effect (P < 0.05, Fig. 4 E–G).

3.5. In vivo knockdown of FPR2 or activation of Rac1 attenuated the neuro-protective effects of RvD1 at 24 h post HI

To investigate whether pathway interventions could influence brain injury, FPR2 was knocked down and Rac1 was activated using siRNA and CRISPR. TTC staining showed that either FPR2 siRNA or Rac1 activation CRISPR significantly reversed the protective effects of RvD1 at 24 h after HI, as seen from the increased percent infarct area in those groups (P < 0.05, Fig. 5 A, B). Consistently, geotaxis test demonstrated that rats treated with RvD1 in combination with either FPR2 siRNA or Rac1 activation CRISPR showed more severe neurological deficits compared with corresponding controls at 24 h after HI (P < 0.05, Fig. 5C).

3.6. RvD1 suppressed inflammation through FPR2/Rac1/NOX2 pathway

Western blot data showed that all downstream target proteins and critical inflammatory cytokines, including GTP-Rac1 (activity of Rac1), total-Rac1, NOX2, IL-1β and TNF-α, were up-regulated in vehicle group when compared with sham group, while RvD1 treated group reversed that effect (P < 0.05, Fig. 6 A–G). FPR2 siRNA significantly decreased FPR2 expression, thereby abolishing the effects of RvD1. FPR2 siRNA intervention significantly reversed the effect of RvD1, evidenced by up-regulated level of GTP-Rac1, total-Rac1, NOX2, IL-1β and TNF-α compared with scramble siRNA group (P < 0.05, Fig. 6 A–G).

To further investigate the potential mechanisms of RvD1, Rac1 activation CRISPR was used. Western blot data showed that expression of GTP-Rac1, total-Rac1, NOX2, IL-1β and TNF-α were significantly increased in HI+Vehicle group when compared with sham group, while RvD1 treatment attenuated the increase (P < 0.05, Fig. 7 A–G). Rac1 CRISPR significantly increased Rac1 activity and expression, which was associated with increased expression of NOX2, IL-1β and TNF-α (P < 0.05, Fig. 7 A–G).

4. Discussion

In the present study, we demonstrated that endogenous FPR2 expression levels were increased while RvD1 decreased at 24 h after HI. Moreover, we found that exogenous RvD1 administration reduced percent infarction area, alleviated both short- and long-term neurological deficits, and attenuated neuroinflammation after HI, which were accompanied by a decrease in the expression of GTP-Rac1, Total-Rac1, NOX2, and also pro-inflammatory factors including IL-1β and TNF-α. In addition, using FPR2 siRNA and Rac1 activation CRISPR we were able to determine that RvD1 exerted its anti-inflammatory effects by binding with FPR2, which then functioned through Rac1/NOX2 pathway. These findings indicated that RvD1 administration improved outcomes after HI at least in part by attenuating neuroinflammation via binding with FPR2 and then interacting with Rac1/NOX2 signaling pathway.

RvD1, a biosynthetic product of ω-3 fatty docosahexaenoic acids (DHA), belongs to a new class of specialized pro-resolving lipid mediators (SPMs) (Cai et al., 2018). Studies have shown that RvD1 is enriched in the brain and synapses (Hong et al., 2007; Weiser et al., 2016). Previous study showed that RvD1 treatment (i.p.) promoted functional recovery and protected against neuroinflammation via a reduction in activated microglia and astrocytes (Bisicchia et al., 2018). However, its role in HI has not yet been explored. Here in we aimed at elucidating the protective roles of RvD1 and its signaling pathway after neonatal HI.

In the present study, we demonstrated for the first time that RvD1 has anti-inflammatory effects in a neonatal HI rat model. Firstly, we evaluated the temporal expression of endogenous RvD1 after HI. The results indicated that RvD1 was decreased significantly at 24 h post HI. This is consistent with recent studies that RvD1 levels were lowered in patients with systemic lupus erythematosus (SLE) or neuromyelitis optica spectrum disorders compared with healthy subjects (Navarini et al., 2018; Wang et al., 2018). Moreover, bone fracture was also reported to decrease levels of RvD1 compared with sham and naive animals (Zhang et al., 2018). However, increased production of RvD1 was found in sham animals of bone fracture. Similar results have also been reported where the protection against transient global cerebral ischemia (just for 20 min) was correlated with increased production of RvD1 (Luo et al., 2014). Based on these results, we speculated that if the injury is mild (such as sham bone fracture and transient ischemia for 20 min), RvD1 would be increased to play a protective role. However, when the injury is severe (for example, bone fracture and HI), the bio-synthesis of RvD1 would be damaged, so its level would be decreased.

FPR2 is a high-affinity receptor for RvD1 and has been shown to be highly expressed in microglia and astrocytes (Guo et al., 2016). Similar to previous findings, we demonstrated that FPR2 was expressed in microglia and astrocytes in the neonatal rat brain. Microglia is a major cell involved in inflammatory processes in the brain and astrocytes are also widely accepted for inflammatory regulation after HI (Ziemka-Nalecz et al., 2017). In our study RvD1 inhibited activation of microglia and astrocytes, and IL-1β release as well, which further confirmed the role of FPR2 in anti-inflammation. Currently, there are also FPR1 and FPR3, however, RvD1 can only bind to FPR2 with high affinity (Gavins, 2010). In our study, we observed that FPR2 siRNA decreased the expression of FPR2 and worsened neurological function after HI, which suggested a beneficial role of FPR2. The expression of FPR2 could be up-regulated in some diseases, such as glioblastomas (GBM), subarachnoid hemorrhage (SAH) (Tadei et al., 2018; Guo et al., 2016). Our results showed that endogenous FPR2 expression increased in a time dependent manner peaking at 24 h after HI. An increase in FPR2 expression may be an effort to strengthen its function after HI, which seems a possible explanation for the increase of FPR2 levels. Additionally our results showed that exogenous RvD1 further increased the expression of FPR2. The results were comparable with previous studies where VIP treatment, Annexin A1 or its mimetic peptide Ac2-26 (Carion et al., 2018; Girol et al., 2013) increased expression of FPR2. We speculate that HI injury may initially activate the inflammatory response and then trigger the reaction of FPR2 signaling to reduce inflammation. This is supported by our data where we showed that RvD1, binding with FPR2, exerted anti-inflammatory effects after HI. Based on our Western blot results, we observed that after RvD1 treatment an increase in FPR2 was

accompanied with a significant reduction in IL-1β and TNF-α expression. To further demonstrate the role of FPR2 in the anti-inflammatory mechanism of RvD1, FPR2 siRNA was administered before HI with RvD1 treatment. The results showed that knockdown of FPR2 abolished the protective effects of RvD1 and reversed the expression of downstream proteins, indicating that FPR2 played an essential role in activating the down-stream anti-inflammatory pathway of RvD1. This treatment aims at activating endogenous resolving inflammatory systems, which is different from inhibiting inflammation occurrence (Norling and Serhan, 2010). Our study is the first to show the protective effects of RvD1 in neonatal rat HI model, which suggests that systemic RvD1 supplementation can be a promising candidate in the treatment of neonatal HI injury and other diseases with similar pathological mechanisms.

Inflammation is a critical process resulting in secondary injury after HI. Although anti-inflammatory effects of RvD1 have been previously reported in many disease models (Zhang et al., 2015; Wang et al., 2014; Bisicchia et al., 2018), the underlying mechanism remains unclear. Here we explored the downstream signaling pathway following FPR2 activation. FPR2 belongs to the G-protein-coup led receptors (GPCR). During activation, G protein dissociates to subunits and activates Rac1. Rac1 is a member of the Rho GTPase family, which functions as molecular switches, cycling between GTP- and GDP-bound states (Wang et al., 2016). GTP-Rac1 is the activated form, and is required for FPR2 activation to exert its anti-inflammatory effects. Our results showed that both GTP-Rac1 and total Rac1 were increased with RvD1 administration after HI. NOX2 has been demonstrated to be Rac1 dependent and is a critical downstream molecule that is activated by RvD1. Previous studies have shown that Rac1 contributes to NOX assembly (Diekmann et al., 1994). In our study, administration of RvD1 significantly increased the expression of NOX2. This finding was similar with a previous report where RvD1 mediated NOX2 inactivation in macrophages (Lee and Surh, 2013). Overall, our results suggested that RvD1 treatment produced anti-inflammatory function by binding to FPR2 and interacting with Rac1/NOX2 pathway in neonatal HI model.

NOX2 is the most important NADPH oxidase mediating cerebral injury (Kahles and Brandes, 2013). Apart from generating reactive oxygen species (ROS), mounting evidence has demonstrated that NOX2 contributed to the pathogenesis of many inflammatory diseases (Benusa et al., 2017; Diebold et al., 2015). Inhibiting NOX2 significantly reduced both microglial activation and cytokines' concentration (Huang et al., 2018). It has been shown that NOX2 knockout mice have less severe post-ischemic inflammation, as evidenced by reduced microglial activation and decreased inflammatory mediators, such as IL-1β and TNF (Chen et al., 2011). Similarly, NOX2 inhibition reduced production of ROS and pro-inflammatory cytokines, concomitant with limited tissue loss and improved functional outcomes in TBI (Kapoor et al., 2018; Kumar et al., 2016; Ma et al., 2018). Moreover, NOX inhibition or global genetic NOX2 knockout suppressed the M1 "pro-inflammatory" profile of microglia/macrophages and simultaneously increased the M2 "anti-inflammatory" profile in the injured brain (Wang et al., 2017). Our study firstly associated NOX2 inactivation with anti-inflammatory receptor FPR2, which not only confirmed the role of NOX2 in inflammation but also showed the upstream signaling pathway of NOX2.

Our data indicated that NOX2 inhibition as a result of upstream FPR2 activation or Rac1 inhibition reduced infarct area and improved geotaxis reflex, while increased NOX2 expression was correlated with enlarged infarct area and worsened neurological function. This seems to be paradoxical with one previous study where although NOX2 expression was increased in the brain of the neonatal mice, neither genetic nor pharmacological inhibition of NADPH oxidase reduced the extent of brain injury (Doverhag et al., 2008). This may be explained due to different species used (neonatal rat versus mice). Furthermore, severity of hypoxia is also different: in that study 60 min hypoxia was used, while in our study hypoxia for 2 h and 30 min. Additionally, it has been reported that NOX2 knockout mice exhibited markedly less retinal neovascularization in P7 mice (Chan et al., 2013), indicating that genetic inhibition of NOX2 could also function in neonatal mice. There are also numerous papers reporting that NOX inhibition has protective effects in neonatal rats. A previous study reported that pretreatment of neonatal rats (P14) with the NOX inhibitor, apocynin, prevented reduction in pavalbumin (PV) immunoreactivity, PV-cells loss in the prefrontal cortex and development of anxiety-like behavior after intermittent hypoxia exposure (Liang et al., 2016). Moreover, NOX2 inhibitor attenuated the cognitive impairments as evidenced by the decreased freezing time to context after ketamine exposure to neonatal rat pups (P6 to P8) (Zhang et al., 2016). A second point that needs to be noted: some studies have shown that consequences of neonatal hypoxic ischemia may be sex-dependent, as demonstrated by males having weaker memory deficits (Dong et al., 2018). Some reasons have been forwarded, such as hormone differences, sex differences in cell death pathways, and sex differences in oxidative stress, although potential mechanisms are still under exploration (Netto et al., 2017). In our experiments, the performance of both sexes were evaluated by foot fault test, rotarod test and water maze. There was no significant difference between genders after HI injury and also no significant difference was seen after RvD1 treatment. This finding may be explained due to different model (left versus right common carotid artery occlusion), different hypoxia exposure duration, and different timing of outcome analysis used in this study. In addition, our results are similar with previous studies where it was demonstrated that CpG-ODN or adiponectin exerted its neuroprotective effect without showing any differences among sexes (Xu et al., 2018; Ye et al., 2018).

5. Conclusion

Our present study showed that treatment with RvD1 reduced percent infarct area, improved neurological function and attenuated inflammation through binding to FPR2 and then interacting with Rac1/NOX2 signaling pathway after hypoxic-ischemic injury in the neonatal rat. Therefore, activation of FPR2 with RvD1 may be a promising therapeutic strategy for treating HIE.

Supplementary Material

Refer to Web version on PubMed Central for supplementary material.

Acknowledgements

Abbreviations:

RvD1   resolvin D1

FPR2   formyl peptide receptor 2

Rac1   Ras-related C3 botulinum toxin substrate 1

NOX2   nicotinamide adenine dinucleotide phosphate (NADPH) oxidase 2

HI   hypoxia-ischemia

Iba1   ionized calcium binding adaptor molecule 1

GFAP   glial fibrillary acidic protein

MPO   myeloperoxidase

IL-1β   interleukin 1β

TNF-α   tumor necrosis factor α

Reference

Acevedo A, González-Billault C, 2018 Crosstalk between Rac1-mediated actin regulation and ROS production. Free Radic. Biol. Med. 116, 101–113. [PubMed: 29330095]

Akbar H, Duan X, Piatt R, Saleem S, Davis AK, Tandon NN, Bergmeier W, Zheng Y, 2018 Small molecule targeting the Rac1-NOX2 interaction prevents collagen-related peptide and thrombin-induced reactive oxygen species generation and platelet activation. J. Thromb. Haemost 16(10), 2083–2096. [PubMed: 30007118]

Benusa SD, George NM, Sword BA, DeVries GH, Dupree JL, 2017 Acute neuroinflammation induces AIS structural plasticity in a NOX2-dependent manner. J. Neuroinflammation 14(1), 116. [PubMed: 28595650]

Bisicchia E, Sasso V, Catanzaro G, Leuti A, Besharat ZM, Chiacchiarini M, Molinari M, Ferretti E, Viscomi MT, Chiurchiú V, 2018 Resolvin D1 halts remote neuroinflammation and improves functional recovery after focal brain damage via ALX/FPR2 receptor-regulated microRNAs. Mol. Neurobiol 55(8), 6894–6905. [PubMed: 29357041]

Cai W, Liu S, Hu M, Sun X, Qiu W, Zheng S, Hu X, Lu Z, 2018 Post-stroke DHA treatment protects against acute ischemic brain injury by skewing macrophage polarity toward the M2 phenotype. Transl. Stroke Res. 9(6), 669–680. [PubMed: 30203370]

Carion TW, Kracht D, Strand E, David E, McWhirter C, Ebrahim AS, Berger EA, 2018 VIP modulates the ALX/FPR2 receptor axis toward inflammation resolution in a mouse model of bacterial keratitis. Prostaglandins Other Lipid Mediat. 140, 18–25. [PubMed: 30529189]

Carrizzo A, Forte M, Lembo M, Formisano L, Puca AA, Vecchione C, 2014 Rac-1 as a new therapeutic target in cerebro- and cardio-vascular diseases. Curr. Drug Targets 15(13), 1231–1246. [PubMed: 25345393]

Chan EC, van Wijngaarden P, Liu GS, Jiang F, Peshavariya H, Dusting GJ, 2013 Involvement of Nox2 NADPH oxidase in retinal neovascularization. Invest. Ophthalmol. Vis. Sci 54(10), 7061–7067. [PubMed: 24106122]

Chen H, Kim GS, Okami N, Narasimhan P, Chan PH, 2011 NADPH oxidase is involved in post-ischemic brain inflammation. Neurobiol. Dis 42(3), 341–348. [PubMed: 21303700]

Chen D, Dixon BJ, Doycheva DM, Li B, Zhang Y, Hu Q, He Y, Guo Z, Nowrangi D, Flores J, Filippov Y, Zhang JH, Tang J, 2018 IRE1a inhibition decreased TXNIP/NLRP3 inflammasome activation through miR-17-5p after neonatal hypoxic-ischemic brain injury in rats. J. Neuroinflammation 15(1), 32. [PubMed: 29394934]

Diebold BA, Smith SM, Li Y, Lambeth JD, 2015 NOX2 as a target for drug development: indications, possible complications, and progress. Antioxid. Redox Signal. 23(5), 375–405. [PubMed: 24512192]

Diekmann D, Abo A, Johnston C, Segal AW, Hall A, 1994 Interaction of Rac with p67phox and regulation of phagocytic NADPH oxidase activity. Science 265(5171), 531–533. [PubMed: 8036496]

Dixon BJ, Reis C, Ho WM, Tang J, Zhang JH, 2015 Neuroprotective strategies after neonatal hypoxic ischemic encephalopathy. Int. J. Mol. Sci 16(9), 22368–22401. [PubMed: 26389893]

Dong S, Zhang Q, Kong D, Zhou C, Zhou J, Han J, Zhou Y, Jin G, Hua X, Wang J, Hua F, 2018 Gender difference in the effect of progesterone on neonatal hypoxic/ischemic brain injury in mouse. Exp Neurol. 306, 190–198. [PubMed: 29772244]

Doverhag C, Keller M, Karlsson A, Hedtjarn M, Nilsson U, Kapeller E, Sarkozy G, Klimaschewski L, Humpel C, Hagberg H, Simbruner G, Gressens R, Savma n K., 2008 Pharmacological and genetic inhibition of NADPH oxidase does not reduce brain damage in different models of perinatal brain injury in newborn mice. Neurobiol. Dis 31(1), 133–144. [PubMed: 18571099]

Fan X, Jiang Y, Yu Z, Liu Q, Guo S, Sun X, van Leyen K, Ning M, Gao X, Lo EH, Wang X, 2017 Annexin A2 plus low-dose tissue plasminogen activator combination attenuates cerebrovascular dysfunction after focal embolic stroke of rats. Transl. Stroke Res. 8(6), 549–559. [PubMed: 28580536]

Fathali N, Ostrowski RP, Hasegawa Y, Lekic T, Tang J, Zhang JH, 2013 Splenic immune cells in experimental neonatal hypoxia-ischemia. Transl. Stroke Res. 4(2), 208–219. [PubMed: 23626659]

Gamdzyk M, Doycheva DM, Malaguit J, Enkhjargal B, Tang J, Zhang JH, 2018 Role of PPAR-p/5/miR-17/TXNTP pathway in neuronal apoptosis after neonatal hypoxic-ischemic injury in rats. Neuropharmacology 140, 150–161. [PubMed: 30086290]

Gavins FN, 2010 Are formyl peptide receptors novel targets for therapeutic intervention in ischaemia-reperfusion injury? Trends Pharmacol. Sci. 31(6), 266–276. [PubMed: 20483490]

Girol AP, Mimura KK, Drewes CC, Bolonheis SM, Solito E, Farsky SH, Gil CD, Oliani SM, 2013 Anti-inflammatory mechanisms of the annexin A1 protein and its mimetic peptide Ac2-26 in models of ocular inflammation in vivo and in vitro. J. Immunol 190(11), 5689–5701. [PubMed: 23645879]

Guo Z, Hu Q, Xu L, Guo ZN, Ou Y, He Y, Yin C, Sun X, Tang J, Zhang JH, 2016 Lipoxin A4 reduces Inflammation through formyl peptide receptor 2/p38 MAPK signaling pathway in subarachnoid hemorrhage rats. Stroke 47(2), 490–497. [PubMed: 26732571]

He HQ., Ye RD, 2017 The formyl peptide receptors: diversity of ligands and mechanism for recognition. Molecules 22(3).

Hong S, Lu Y, Yang R, Gotlinger KH, Petasis NA, Serhan CN, 2007 Resolvin D1, protectin D1, and related docosahexaenoic acidderived products: analysis via electrospray/low energy tandem mass spectrometry based on spectra and fragmentation mechanisms. J. Am. Soc. Mass. Spectrom 18(1), 128–144. [PubMed: 17055291]

Huang WY, Lin S, Chen HY, Chen YP, Chen TY, Hsu KS, Wu HM, 2018 NADPH oxidases as potential pharmacological targets against increased seizure susceptibility after systemic inflammation. J. Neuroinflammation 15(1), 140. [PubMed: 29753328]

Jiang B, Li L, Chen Q, Tao Y, Yang L, Zhang B, Zhang JH, Feng H, Chen Z, Tang J, Zhu G, 2017 Role of glibenclamide in brain injury after intracerebral hemorrhage. Transl. Stroke Res. 8(2), 183–193. [PubMed: 27807801]

Kahles T, Brandes RP, 2013 Which NADPH oxidase isoform is relevant for ischemic stroke? The case for nox 2. Antioxid. Redox Signal. 18(12), 1400–1417. [PubMed: 22746273]

Kapoor M, Sharma N, Sandhir R, Nehru B, 2018 Effect of the NADPH oxidase inhibitor apocynin on ischemia-reperfusion hippocampus injury in rat brain. Biomed. Pharmacother 97, 458–472. [PubMed: 29091896]

Kumar A, Barrett JP, Alvarez-Croda DM, Stoica BA, Faden AI, Loane DJ, 2016 NOX2 drives Ml-like microglial/macrophage activation and neurodegeneration following experimental traumatic brain injury. Brain Behav. Immun. 58, 291–309. [PubMed: 27477920]

Kurinczuk JJ, White-Koning M, Badawi N, 2010 Epidemiology of neonatal encephalopathy and hypoxic-ischaemic encephalopathy. Early Hum. Dev. 86(6), 329–338. [PubMed: 20554402]

Lapchak PA, Zhang JH, 2017 The high cost of stroke and stroke cytoprotection research. Transl. Stroke Res. 8(4), 307–317. [PubMed: 28039575]

Lee HN, Surh YJ, 2013 Resolvin D1-mediated NOX2 inactivation rescues macrophages undertaking efferocytosis from oxidative stress-induced apoptosis. Biochem. Pharmacol 86(6), 759–769. [PubMed: 23856291]

Liang D, Li G, Liao X, Yu D, Wu J, Zhang M, 2016 Developmental loss of parvalbumin-positive cells in the prefrontal cortex and psychiatric anxiety after intermittent hypoxia exposures in neonatal rats might be mediated by NADPH oxidase-2. Behav. Brain Res. 296, 134–140. [PubMed: 26319087]

Luo C, Ren H, Wan JB, Yao X, Zhang X, He C, So KF, Kang JX, Pei Z, Su H, 2014 Enriched endogenous omega-3 fatty acids in mice protect against global ischemia injury. J. Lipid Res. 55(7), 1288–1297. [PubMed: 24875538]

Ma MW, Wang I, Dhandapani KM, Wang R, Brann DW, 2018 NADPH oxidases in traumatic brain injury - Promising therapeutic targets? Redox Biol. 16, 285–293. [PubMed: 29571125]

McAdams RM, Juul SE, 2016 Neonatal encephalopathy: update on therapeutic hypothermia and other novel therapeutics. Clin. Perinatal. 43(3), 485–500.

Navarini L, Bisogno X, Margiotta DPE, Piccoli A, Angeletti S, Laudisio A, Ciccozzi M, Afeltra A, Maccarrone M, 2018 Role of the specialized proresolving mediator resolvin D1 in systemic lupus erythematosus: preliminary results. J. Immunol. Res 2018, 5264195. [PubMed: 30420970]

Netto CA, Sanches E, Odorcyk FK, Duran-Carabali LE, Weis SN, 2017 Sex-dependent consequences of neonatal brain hypoxia-ischemia in the rat. J Neurosci Res. 95(1–2), 409–421. [PubMed: 27870406]

Norling LY, Serhan CN, 2010 Profiling in resolving inflammatory exudates identifies novel anti-inflammatory and pro-resolving mediators and signals for termination. J. Intern. Med 268(1), 15–24. [PubMed: 20497301]

Pang J, Peng J, Matei N, Yang P, Kuai L, Wu Y, Chen L, Vitek MP, Li F, Sun X, Zhang JH, Jiang Y, 2018 Apolipoprotein E exerts a whole-brain protective property by promoting Ml? microglia quiescence after experimental subarachnoid hemorrhage in mice. Transl. Stroke Res. 9(6), 654–668. [PubMed: 30225551]

Parikh P, Juul SE, 2018 Neuroprotective strategies in neonatal brain injury. J. Pediatr 192,22–32. [PubMed: 29031859]

Peshavariya HM, Taylor CJ, Goh C, Liu GS, Jiang F, Chan EC, Dusting GJ, 2013 Annexin peptide Ac2-26 suppresses TNFα-induced inflammatory responses via inhibition of Rac1-dependent NADPH oxidase in human endothelial cells. Plos One 8(4), e60790. [PubMed: 23637767]

Raz L, Zhang QG, Zhou CF, Han D, Gulati P, Yang LC, Yang F, Wang RM, Brann DW, 2010 Role of Rac1 GTPase in NADPH oxidase activation and cognitive impairment following cerebral ischemia in the rat. PLoS One 5(9), e12606. [PubMed: 20830300]

Serhan CN, Chiang N, 2008 Endogenous pro-resolving and anti-inflammatory lipid mediators: a new pharmacologic genus. Br. J. Pharmacol 153 Suppl. 1, S200–215. [PubMed: 17965751]

Tadei MB, Mayorquim MV, de Souza CB, de Souza Costa S, Possebon L, Souza HR, Iyomasa-Pilon MM, Geromel MR, Girol AP, 2018 Expression of the Annexin A1 and its correlation with matrix metalloproteinases and the receptor for formylated peptide-2 in diffuse astrocytic tumors. Ann. Diagn. Pathol 37, 62–66. [PubMed: 30286327]

Tuttolomondo A, Di Raimondo D, di Sciacca R, Pinto A, Licata G, 2008 Inflammatory cytokines in acute ischemic stroke. Curr. Pharm. Des 14(33), 3574–3589. [PubMed: 19075734]

Wang Q, Zheng X, Cheng Y, Zhang YL, Wen HX, Tao Z, Li H, Hao Y, Gao Y, Yang LM, Smith FG, Huang CJ, Jin SW, 2014 Resolvin D1 stimulates alveolar fluid clearance through alveolar epithelial sodium channel, Na,K-ATPase via ALX/cAMP/PI3K pathway in lipopolysaccharide-induced acute lung injury. J. Immunol 192(8), 3765–3777. [PubMed: 24646745]

Wang Y, Xu X, Pan M, Jin X, 2016 ELMO1 directly interacts with Gβγ subunit to transduce GPCR signaling to Rac1 activation in chemotaxis. J. Cancer 7(8), 973–983. [PubMed: 27313788]

Wang J, Ma MW, Dhandapani KM, Brann DW, 2017 Regulatory role of NADPH oxidase 2 in the polarization dynamics and neurotoxicity of microglia/macrophages after traumatic brain injury. Free Radic. Biol. Med. 113, 119–131. [PubMed: 28942245]

Wang X, Jiao W, Lin M, Lu C, Liu C, Wang Y, Ma D, Wang X, Yin P, Feng J, Zhu J, Zhu M, 2018 Resolution of inflammation in neuromyelitis optica spectrum disorders. Mult. Scler. Relat. Disord 27,34–41. [PubMed: 30300851]

Weiser MJ, Butt CM, Mohajeri MH, 2016 Docosahexaenoic acid and cognition throughout the lifespan. Nutrients 8(2), 99. [PubMed: 26901223]

Xu N, Zhang Y, Doycheva DM, Ding Y, Zhang Y, Tang J, Guo H, Zhang JH,2018 Adiponectin attenuates neuronal apoptosis induced by hypoxia-ischemia via the activation of AdipoRl/APPLl/LKBl/AMPK pathway in neonatal rats. Neuropharmacology. 133,415–428. [PubMed: 29486166]

Ye L, Feng Z, Doycheva D, Malaguit J, Dixon B, Xu N, Zhang JH, Tang J, 2018 CpG-ODN exerts a neuroprotective effect via the TLR9/pAMPK signaling pathway by activation of autophagy in a neonatal HIE rat model. Exp. Neurol 301(Pt A), 70–80. [PubMed: 29274721]

Zhang T, Shu HH, Chang L, Ye E, Xu KQ, Huang WQ, 2015 Resolvin D1 protects against hepaticischemia/reperfusioninjury in rats.Int. Immunopharmacol 28(1), 322–327. [PubMed: 26118631]

Zhang H, Sun XR, Wang J, Zhang ZZ, Zhao HT, Li HH, Ji MH, Li KY, Yang JJ, 2016 Reactive oxygen species-mediated loss of phenotype of parvalbumin interneurons contributes to long-term cognitive impairments after repeated neonatal ketamine exposures. Neurotox. Res 30(4), 593–605. [PubMed: 27443555]

Zhang L, Terrando N, Xu ZZ, Bang S, Jordt SE, Maixner W, Serhan CN, Ji RR, 2018 Distinct analgesic actions of DHA and DHA-Derived specialized pro-resolving mediators on post-operative pain after bone fracture in mice. Front Pharmacol. 9, 412. [PubMed: 29765320]

Ziemka-Nalecz M, Jaworska J, Zalewska X, 2017 Insights into the neuroinflammatory responses after neonatal hypoxia-ischemia. J. Neuropathol. Exp. Neurol. 76(8), 644–654. [PubMed: 28789477]

Highlights

- Endogenous FPR2 expression levels were increased while RvD1 decreased after HI.

- RvD1 treatment reduced percent infarction area and improved neurological function.

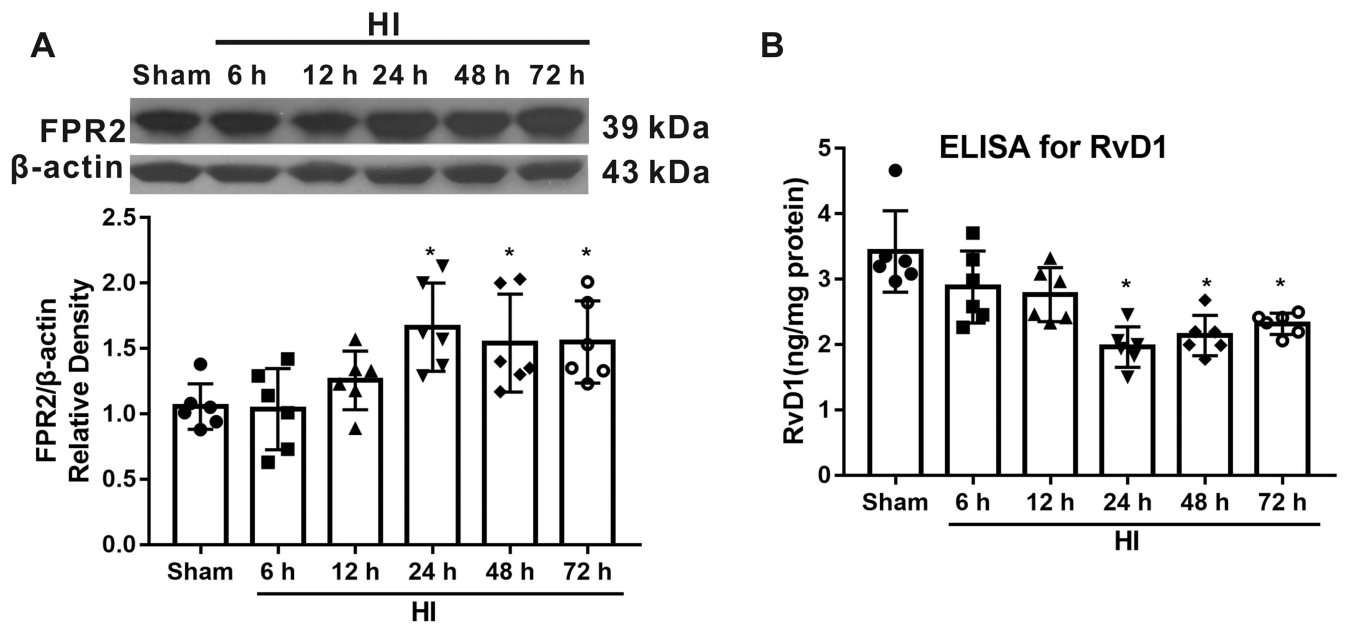- RvD1 binding with FPR2 attenuated inflammation through Rac1/NOX2 pathway.

Fig. 1.
Time course expression of FPR2 and RvD1 post hypoxia-ischemia (HI). (A) Representative Western blot bands and schematic diagram showed that FPR2 levels increased after HI, reaching significance from 24 h to 72 h. (B) RvD1 was decreased after HI. ANOVA followed by Tukey test was used for analysis. Data are presented as mean ± SD, n=6. * P<0.05 vs. sham. RvD1, resolvin D1.

Fig. 2.
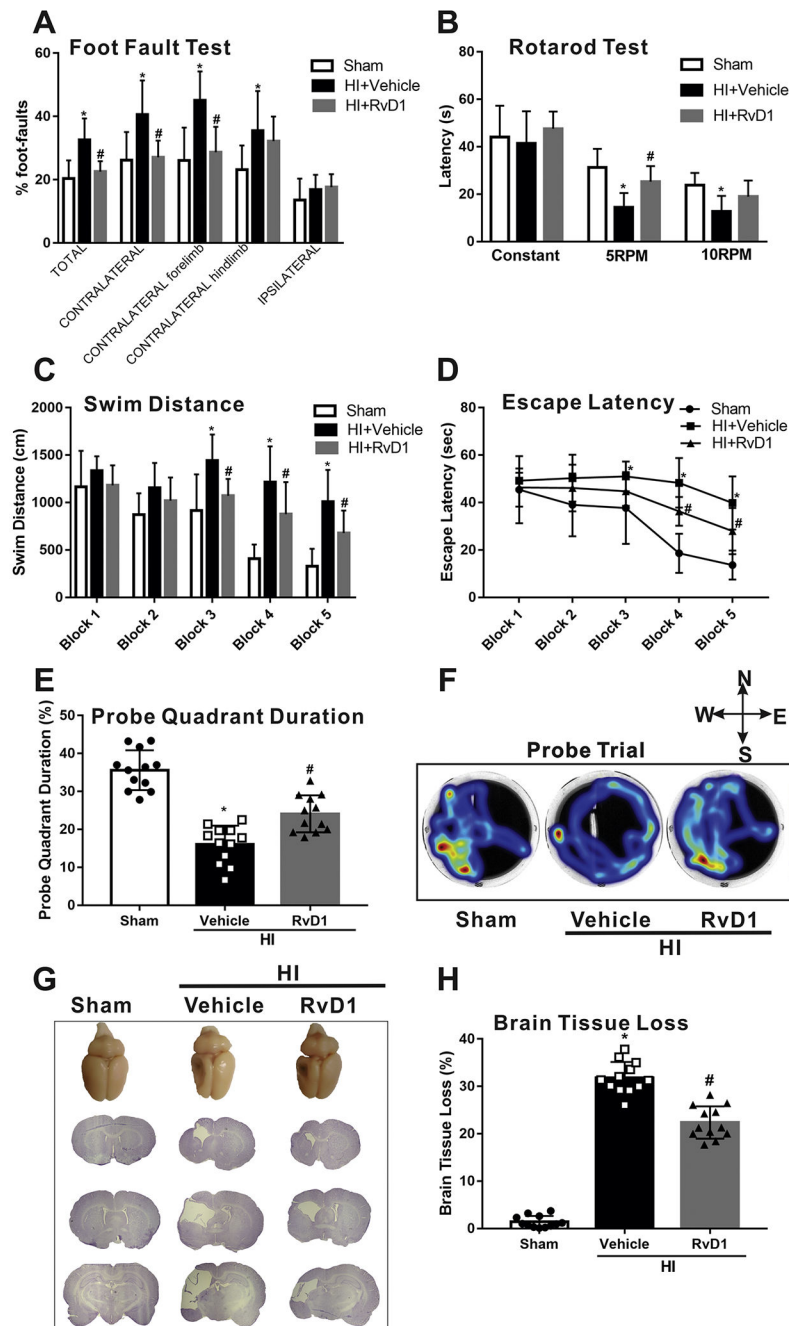Effects of RvD1 (different doses) on infarct area, geotaxis reflex and weight loss at 24 h post hypoxia-ischemia (HI). Representative TTC stained brain sections (A) and schematic diagram (B) showed that RvD1 treatment (5 μg/kg and 15 μg/kg) significantly reduced percent infarction area after HI. (C and D) RvD1 at the dose of 5 μg/kg and 15 μg/kg significantly improved neurological function and reduced weight loss compared with vehicle group. ANOVA followed by Tukey test was used for analysis. Data are presented as mean ± SD, n=6. *P<0.05 vs. sham, # P < 0.05 vs. HI+vehicle. RvD1, resolvin D1.

Fig. 3.
Effects of RvD1 on neurological function and brain tissue loss at 4 weeks post hypoxia-ischemia (HI). Compared with vehicle, RvD1 treatment group alleviated long term neurological deficits, including foot fault test (A), rotarod test (B), swimming distance to find the platform (C), escape latency (D) and time spent in the target quadrant (E). (F) Representative pictures of swim track in Probe Trial. (G) Representative pictures of Nissl's stained brain slices and schematic diagram (H) showed that RvD1 treatment significantly reduced the percent of tissue loss when compared with vehicle. ANOVA followed by Tukey

test was used for analysis. Data were shown as mean ± SD (n=12 per group). * P < 0.05 vs. sham; # P < 0.05 vs. HI+vehicle. RvD1, resolvin D1.
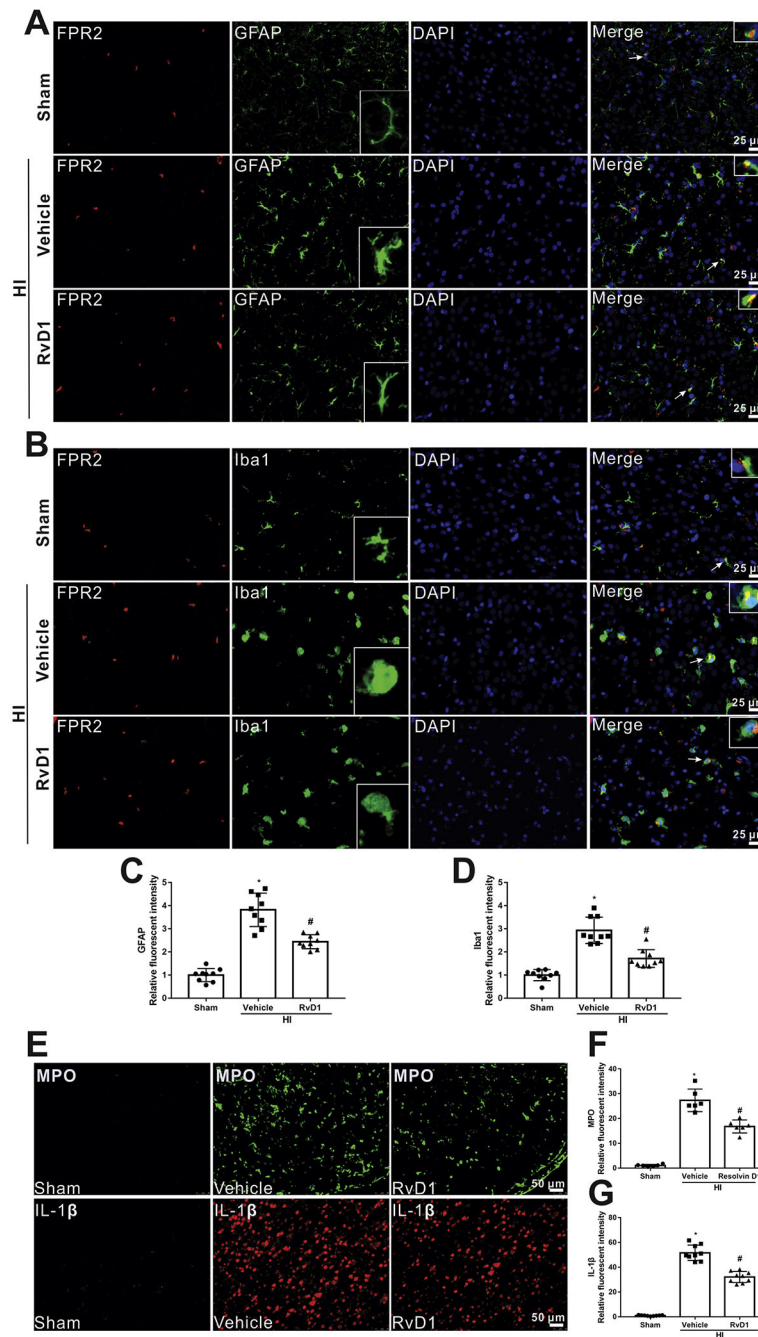
Fig. 4.
Localization of FPR2 and Iba1 (microglial marker) and GFAP (astrocytic marker) in the brain at 24 h post hypoxia-ischemia (HI). (A and B) Immunofluorescent staining showed that FPR2 was co-localized with Iba1 and GFAP. Scale bar=25 μm. (C and D) Quantitative analysis showed that more Iba1 and GFAP were expressed in HI+vehicle group, while RvD1 attenuated the increase. Representative pictures and schematic diagram showed there was more inflammation in vehicle group compared to sham, indicative by positive MPO and IL-1β (E-G), however, RvD1 treatment reduced the increase (E-G). ANOVA followed by

Tukey test was used for analysis. Data were shown as mean ± SD (n=3 per group). * P < 0.05 vs. sham; # P < 0.05 vs. HI+vehicle. RvD1, resolvin D1.
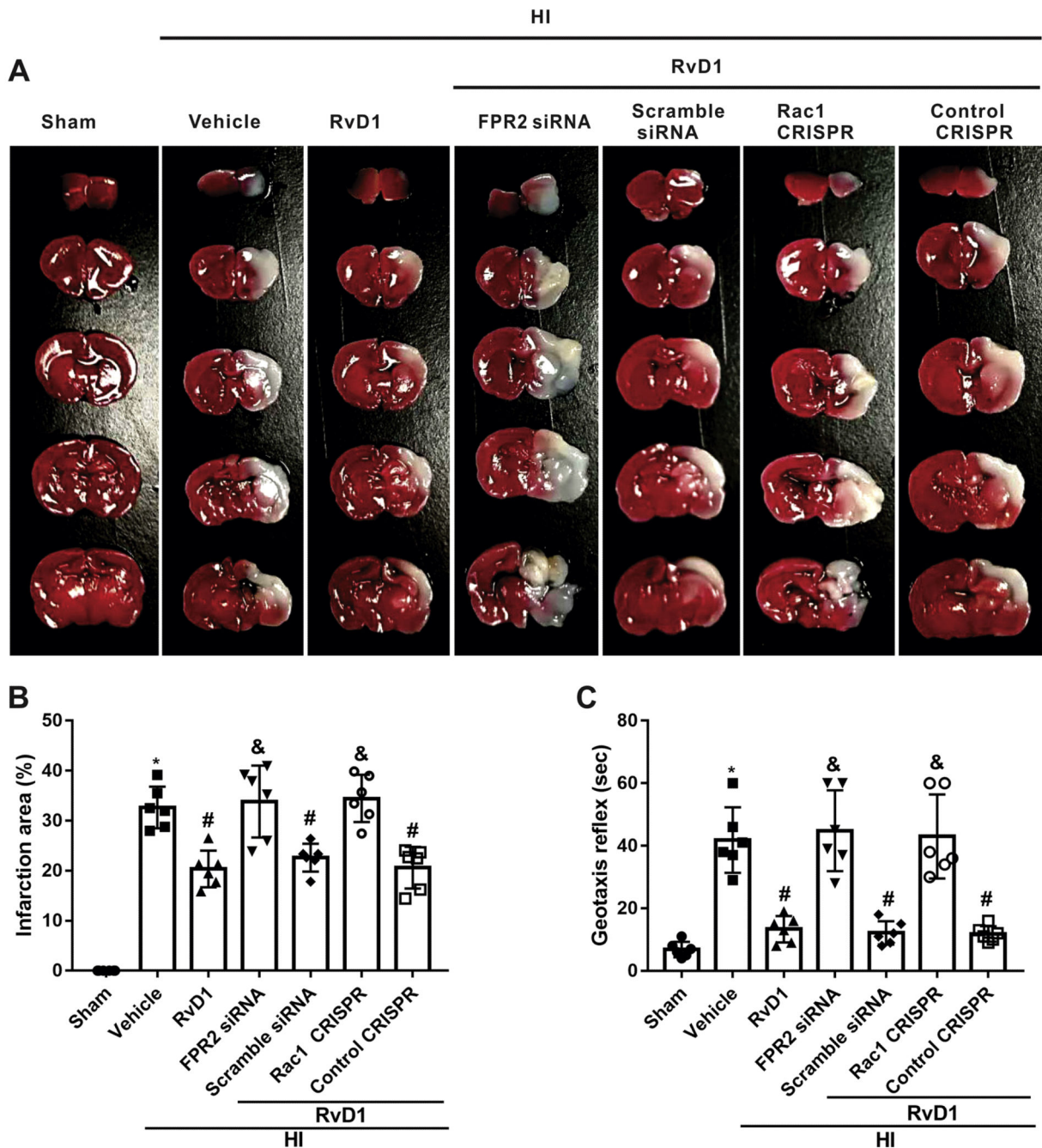
Fig. 5.
Effects of FPR2 siRNA and Rac1 activation CRISPR on infarct area and geotaxis reflex at 24 h post hypoxia-ischemia (HI). (A and B)The infarction area was significantly enlarged with FPR2 siRNA/Rac1 activation CRISPR interventions when compared with respective controls. (C) Interventions with FPR2 siRNA or Rac1 activation CRISPR significantly worsened geotaxis reflex compared with respective controls. ANOVA followed by Tukey test was used for analysis. Data were shown as mean ± SD (n=6 per group). * $P < 0.05$ vs.
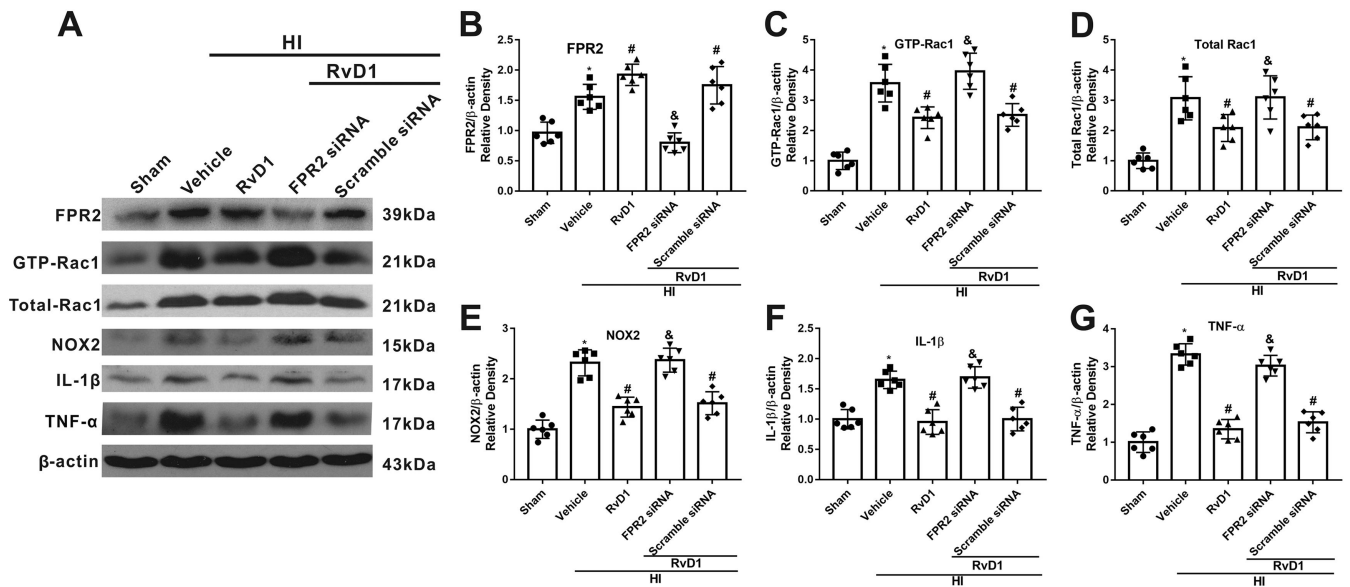
sham group; # P < 0.05 vs. HI+vehicle group, & P < 0.05 vs. HI+RvD1+scramble siRNA group, @ P < 0.05 vs. control CRISPR. RvD1, resolvin D1.
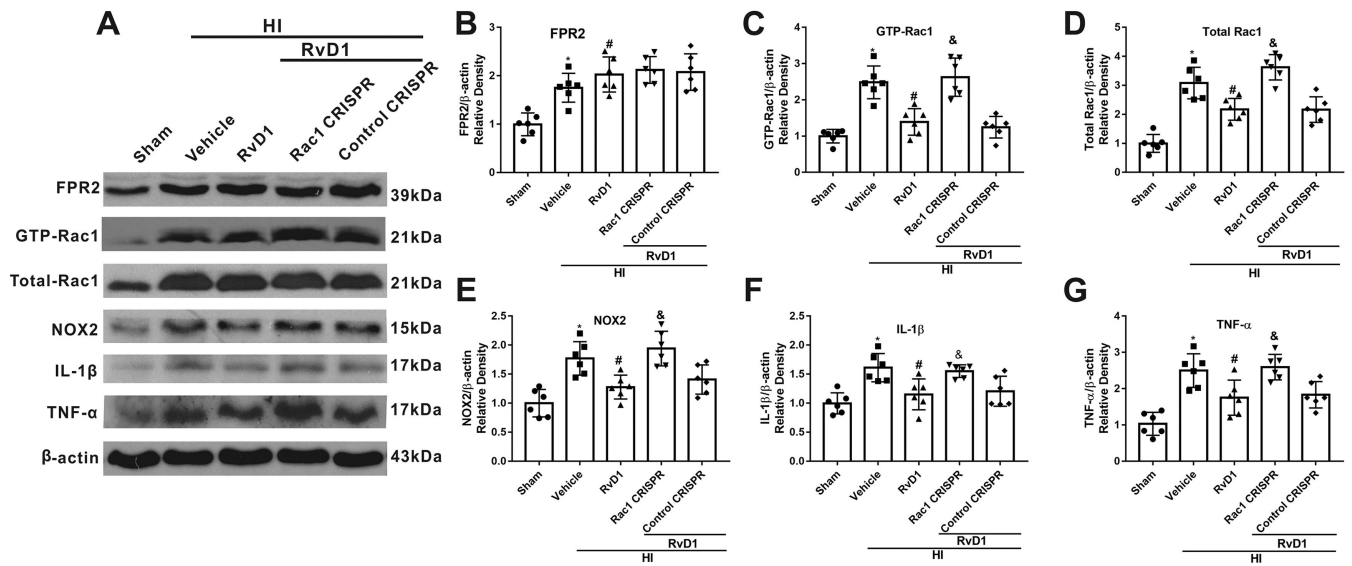
Fig. 6.
Knockdown of FPR2 reduced the anti-inflammation effect of RvD1 at 24 h post hypoxia-ischemia (HI). (A) Representative Western blot bands. (B-G) Quantification of Western blot bands showed that RvD1 significantly increased the expression of FPR2 (B), whereas decreased the expression of GTP-Rac1 (C), total Rac1(D), NOX2(E), IL-1β (F), and TNF-α(G) compared with HI+vehicle group. However, FPR2 siRNA reversed the effect of RvD1 compared with HI+RvD1+scramble siRNA group. ANOVA followed by Tukey test was used for analysis. Data were shown as mean ± SD (n=6 per group). * $P < 0.05$ vs. sham group; # $P < 0.05$ vs. HI+vehicle group; & $P < 0.05$ vs. HI+RvD1+scramble siRNA group. RvD1, resolvin D1.

Fig. 7.

Activation of Rac1 decreased the anti-inflammation function of RvD1 at 24 h post hypoxia-ischemia (HI). (A) Representative Western blot bands. (B-G) Quantification of Western blot bands showed that Rac1 activation CRISPR inhibited the effect of RvD1 on decreasing the expression of GTP-Rac1 (C), total Rac1 (D), NOX2 (E), IL-1β (F), and TNF-α(G) compared with HI+RvD1+control CRISPR. ANOVA followed by Tukey test was used for analysis. Data were shown as mean ± SD (n=6 per group). * P < 0.05 vs. sham group; # P < 0.05 vs. HI+vehicle group; & P < 0.05 vs. HI+RvD1+control CRISPR group. RvD1, resolvin D1.